

# ADOPT: A system for Alerting Drivers to Occluded Pedestrian Traffic

Abrar Alali<sup>\*†</sup>, Stephan Olariu<sup>\*</sup>, Shubham Jain<sup>‡</sup>

<sup>\*</sup> Old Dominion University

aalal003@odu.edu, olariu@cs.odu.edu

<sup>†</sup> Saudi Electronic University

a.alali@seu.edu.sa

<sup>‡</sup> Stony Brook University

jain@cs.stonybrook.edu

**Abstract**—Recent statistics reveal an alarming increase in accidents involving pedestrians (especially children) crossing the street. A common philosophy of existing pedestrian detection approaches is that this task should be undertaken by the moving cars<sup>1</sup> themselves. In sharp departure from this philosophy, we propose to enlist the help of cars parked along the sidewalk to detect and protect crossing pedestrians. In support of this goal, we propose ADOPT: a system for Alerting Drivers to Occluded Pedestrian Traffic. ADOPT lays the theoretical foundations of a system that uses parked cars to: (1) detect the presence of a group of crossing pedestrians – a crossing cohort; (2) predict the time the last member of the cohort takes to clear the street; (3) send alert messages to those approaching cars that may reach the crossing area while pedestrians are still in the street; and, (4) show how approaching cars can adjust their speed, given several simultaneous crossing locations. Importantly, in ADOPT all communications occur over very short distances and at very low power. Our extensive simulations using SUMO-generated pedestrian and car traffic have shown the effectiveness of ADOPT in detecting and protecting crossing pedestrians.

**Index Terms**—Vehicle-to-Vehicle communications, Vehicle-to-Pedestrian communications, pedestrian safety, driver assistance.

## I. INTRODUCTION AND MOTIVATION

According to the National Highway Traffic Safety Administration, 6,301 pedestrians were hit and killed by drivers in the first half of 2021, a 17% increase over 2020<sup>2</sup> [1]. A recent study [2] concluded that one of the main causes of crashes involving pedestrians is occlusion: the driver is unaware of the presence of pedestrians because some object partially or fully occludes them. Therefore, detecting occluded pedestrians reliably and in a timely manner is key to promoting pedestrian safety. For comprehensive survey papers that discuss the effectiveness of various approaches to improving pedestrian safety, we refer the reader to [3] and [4].

A glance at the recent literature reveals an increasing number of publications that leverage the on-board sensing and communication capabilities of present-day cars to heighten the drivers' awareness of surrounding pedestrians. On-board cameras, short- and long-range laser devices, and LiDAR are part

of the arsenal of sensors employed to detect pedestrians [5]. One common characteristic of these sensors is that they require Line-of-Sight (LoS) to enable detection [6]. Because of this, partially or totally occluded pedestrians go undetected most of the time [7]. In addition to the LoS challenge, weather and lighting conditions (e.g., glinting sun or other reduced visibility conditions) are apt to thwart the ability of on-board sensors to detect pedestrians [8], [9], [10].

One approach for detecting pedestrians that does not require LoS involves leveraging wireless communication technologies such as WiFi, DSRC, or short-range technologies such as Zigbee or Bluetooth. While this approach mitigates the LoS challenge, it has serious scalability problems. Indeed, reporting pedestrians within a large radio coverage area tends to be unreliable due to known impairments of radio transmission, various forms of interference, message propagation delays, and security concerns [11].

Recently, researchers have suggested supplementing the data collected by on-board sensors with information collected by pre-deployed roadside infrastructure [12]. Aligned with this idea, several projects have been implemented at signalized intersections to promote pedestrian safety [13]. These projects involve installing sensors, cameras, and communication units in roadside infrastructure, such as light poles, to detect pedestrians and to alert approaching cars [14]. Although this approach enables the detection of occluded pedestrians, it focuses on signalized intersections, while the majority of pedestrian accidents tend to occur mid-block [15], [16], [17]. Moreover, this approach is problematic since roadside infrastructure may not be available when needed [10].

Recently, the potential of using parked vehicles as alternative road-side infrastructure in support of sensing and networking has been recognized by a number of researchers. For example, [18] and [19] suggested that by networking cars parked along the sidewalk, the task of relaying messages and other networking tasks can be significantly enhanced.

More recently, it was suggested to aggregate information collected by several moving vehicles in an effort to enable a *collaborative perception* of surrounding pedestrians [8]. The idea is that when a moving vehicle has a LoS connection to a group of pedestrians, it alerts neighboring vehicles, making them aware of the presence of potentially occluded

Research funded by the NSF grant CNS-1951789 and CNS-2106594.

<sup>1</sup>In this work we refer to vehicles simply as cars.

<sup>2</sup>The report accounted for the effects of COVID-19 pandemic.

pedestrians. Alternatively, using Vehicle-to-Pedestrian (V2P) communications [12], the pedestrians are alerted to the presence of approaching cars by pushing messages to their handheld or wearable devices. Collaborative perception is a promising technology for enhancing pedestrian safety. However, in order to work effectively, the collaborative pedestrian detection methodology requires sophisticated sensing resources and communication protocols and may not scale well to a large number of pedestrians [20]. Furthermore, it is rather inaccurate since it relies on inaccurate GPS coordinates to estimate the distance between the pedestrian detected and the vehicle, not to mention the potentially high power consumption [21]. Most importantly, the alert messages sent via DSRC can easily overwhelm the network with unnecessary alerts [22].

#### A. Our contributions

The underlying design philosophy of all the approaches mentioned above is that pedestrian detection should be undertaken by *moving cars* with all the complications that this entails. In sharp departure from this philosophy, we propose *ADOPT: a system for Alerting Drivers to Occluded Pedestrian Traffic* that runs on cars *parked* along the sidewalk.

By design, ADOPT is a low-power system whose stated goal is to alert approaching vehicles to the presence of possibly occluded pedestrians in the street. To implement this functionality, in ADOPT, all communications occur over very short distances and at very low power. Piezo-electric cells implanted in pedestrians' shoes power rudimentary radio transmitters that operate by closing a circuit as the pedestrian's shoe touches the ground. The resulting signals (essentially, radio noise) allow low-power transceivers, installed close to the four corners of parked cars, and integrated into the Controller Area Network (CAN) intra-vehicle network [23], to classify pedestrians as *on the sidewalk* or *in the street*. As long as the pedestrians stay on the sidewalk, ADOPT remains in a low-power vigilant state. When one or several pedestrians step into the street, ADOPT wakes up, locates the crossing pedestrians (a.k.a. crossing cohort), and estimates the time it takes the last member of the cohort to cross the street. By multi-hopping this information through a chain of parked cars along the sidewalk, ADOPT shares with the drivers of approaching cars (a) the location, on a digital map, of the crossing cohort ahead of them; and, (b) the estimated time it takes the cohort to cross the street.

To summarize, the main contributions of ADOPT are related to pedestrian safety and driver assistance. Specifically, this paper:

- 1) provides the theoretical foundations of a low-power and infrastructure-free occluded pedestrian detection system;
- 2) introduces a novel criterion for the classification of pedestrians as "on the sidewalk" or "in the street";
- 3) offers a scheme for estimating the expected time it takes the crossing cohort to clear the street;
- 4) provides an algorithm that allows approaching cars to adjust dynamically their speed, given several simultaneous crossing locations.

The remainder of this work is structured as follows: Section II offers a succinct survey of relevant recent work.

Section III establishes terminology and discusses system assumptions. A detailed discussion of how ADOPT works can be found in Sections IV–VII. Specifically, Section IV offer the details of pedestrian classification and localization. Section V offers the details of the way ADOPT estimates the time it takes a cohort to cross the street. Next, Section VI discusses the details of propagating alert message to alert approaching cars. In Section VII we present an algorithm that can be used by approaching cars to adjust their speed as a result of receiving information about one or several crossing cohorts. The empirical evaluation of ADOPT spans Sections VIII and IX. Specifically, Section VIII introduces the simulation model and the noise model assumed. Our comprehensive simulation results are presented and discussed in Section IX. Finally, Section X offers concluding remarks and maps out directions for future work.

## II. RELEVANT RELATED WORK

The main goal of this section is to offer a succinct overview of the latest pedestrian detection systems and relevant emerging technologies.

#### A. On-board LoS sensors

The literature on pedestrian detection by vehicle's on-board sensors is quite vast [3], [5], [6], [7], [24], [25], [26], [27], [28], [29], [30], [31]. On-board cameras can detect pedestrians only if they fully appear in the view. However, if they are partially occluded, additional effort is needed to recognize them. In a series of papers, [31] have used machine learning to detect partially occluded pedestrians from an on-board camera. Convolutional neural networks were utilized in the detection of partially occluded pedestrians [32], [26], [29].

Sensor fusion approaches have been leveraged to detect occluded pedestrians. Recently, [33], [30] uses on-board thermal infrared sensors to detect pedestrians in low lighting conditions. [28], [27] suggested fusing on-board camera input with LIDAR and thermal sensors to detect pedestrians in low-visibility conditions.

While on-board LoS sensors can detect partially occluded pedestrians, fully occluded pedestrians cannot be detected using the same sensors. Furthermore, relying on LoS sensors for occluded pedestrian detection must involve extensive vision algorithms that may not perform the task in a timely manner.

#### B. V2P and P2V communications

In order to mitigate the problem of occluded pedestrian detection with LoS sensors, Vehicle-to-Pedestrians (V2P) wireless communication was leveraged to detect the presence of pedestrians. WiFi, Zigbee, and Ultra-Wideband UWB were used in [34], [35], [36], [37], [38] for V2P communication and alerting either drivers or pedestrians about anticipated collisions.[39] have proposed a framework for V2P communications via DSRC units with the goal of alerting both the pedestrians and the vehicle to a possible collision. The fusion of the car's perception and V2P communications was leveraged by [40]. Their solution relies on recognizing the

occlusion by a moving vehicle and sending an alert to the pedestrian's device if detected via V2P communications.

Although V2P communications enhance the safety of occluded pedestrians by improving the detection rate, their main drawback is that they are usually power-hungry and are apt to drain the battery of the pedestrian's device if used for extended periods of time. Yet another drawback is that V2P communications rely on inaccurate GPS readings to determine the distance between the pedestrian and approaching vehicles. Additionally, V2P communications do not scale well when multiple pedestrians are found in the street.

### C. Collaborative perception

Collaborative perception in Vehicular Ad Hoc Networks (VANET) is used in pedestrian safety systems when a moving car fails to detect pedestrians using its on-board sensors and relies on remote sensors such as other cars' on-board cameras or street monitoring cameras to provide additional perception. [41] proposed a collaborative system that shares pedestrians' information when they are detected by another car's camera. The detecting car exchanges pedestrian location and speed with the blinded car(s). Their system has the advantage of enabling collaboration between cars to prevent pedestrian/car collisions.

Several projects attempt to enhance pedestrian detection at intersections by installing cameras and ranging sensors on light poles or RSUs. Once the pedestrians are detected, approaching vehicles are alerted to their presence. For example, [42], [43], [44] installed a camera in an RSU to detect pedestrians and to alert approaching vehicles. [45] and [46] suggested fusing input from installed cameras with thermal and LiDAR sensors to detect pedestrians at day and night. In lower cost mechanism, [47] installed piezoelectric elements at the beginning and end of crossing lines to detect pedestrians and to alert approaching vehicles through RSUs. Similarly, [48] suggested placing wireless sensor units on the roadside to detect the presence of pedestrians and to send the detection information to a nearby RSU to share it with the incoming vehicles. The aforementioned approaches are expensive to deploy and, consequently, municipalities usually do not have the resources to install them at all locations. Besides, they only cover controlled intersections while many pedestrians are known to roads mid-block. Additionally, the alert messages are exchanged between RSU and approaching vehicles via DSRC which covers a large area causing network load and impairments of radio transmissions, various forms of interference, message propagation delays, and security concerns.

### D. Putting parked cars to work

Parked cars have been used in VANET as relays for safety message dissemination in areas with low traffic density. As an example, [49] proposed the idea of using parked cars as RSUs to improve VANET connectivity. Similarly, [18] showed that parked cars are useful to work as relay nodes in support of VANET communications. To increase road safety, [19] proposed that parked cars communicate with their moving

counterparts as relay nodes to increase safety in low-density areas by multi-hopping the Cooperative Awareness Messages.

Due to the vast panoply of their on-board sensors, parked cars can also be used as a sensing resource. [50] showed that parked cars can be used as sensing resources and that the CAN bus can be used to provide power to the sensors. Parked cars have been also used for detecting missing objects by [51] by instrumenting cars with RFID readers to detect tags attached to missing objects, then share the detection information with administrative centers. One of the RFID detection approach's drawbacks is that it needs a secure communication medium to protect users' privacy. Undoubtedly, using parked cars as a sensing resource is beneficial in terms of providing accurate and timely information.

### E. Energy harvesting wearables

Energy harvesters such as piezoelectric elements were used in shoes to activate sensors from mechanical energy generated during walking [52]. Moreover, [53] developed a shoe module that can communicate with a smartphone held by the user. Their work showed that the power produced by a single shoe is sufficient to transmit data from a Bluetooth module to the smartphone. Such a module can be used to enable pedestrians to generate signals to be received by nearby receivers that operate on the same frequency as we proposed in this paper. Most importantly, they can transmit signals while consuming power from their motion rather than external batteries.

### F. Short-range RSS localization

Received Signal Strength (RSS) ranging approaches are commonly used in wireless localization techniques for their simplicity and efficiency in terms of power consumption [54]. However, because of its limited accuracy, RSS-based ranging is used mostly as a coarse-grain indicator, especially in long-range localization efforts. As pointed out by [55], the accuracy of RSS localization is surprisingly good at short ranges (within 1-3 meters) which makes it a good candidate to be used in ADOPT.

## III. ADOPT: SYSTEM ASSUMPTIONS

The main goal of this section is to spell out the basic system assumptions that underlie ADOPT.

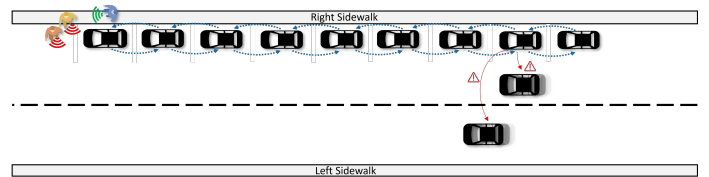


Fig. 1: Illustrating ADOPT: Parked cars detect occluded crossing pedestrians and alert approaching cars.

ADOPT relies on detecting radio frequency (RF) signals transmitted at each step while a pedestrian is walking. Many wearable devices, including smart-phones, wrist-bands, and shoes can detect human steps [56]. Since we aim to design

a low-power and low-cost system, we focus on leveraging wearables that harvest energy from body motion. Specifically, we assume that the pedestrians (who might be children) are wearing shoes fitted with piezoelectric elements that provide a robust, lightweight, and inexpensive source of power for an in-shoe, battery-free, power generator [52], [53]. As already mentioned, when a pedestrian's shoe touches the ground, a circuit is closed and a rudimentary transmitter embedded in the pedestrian's shoe is activated for a fraction of a second.

We assume that the parked cars know their exact geographic location by interfacing with a digital map. In support of detecting the presence of pedestrians, cars are fitted with four low-power radio transceivers placed on the front and rear axles on each side of the car. These transceivers detect and measure the strength of RF signals transmitted by pedestrians' shoes. The four transceivers mentioned above, are integrated into, powered by, and synchronized to the intra-vehicle CAN bus [23].

The cars parked along the sidewalk are assumed to be aware of the distance between their right transceivers and the sidewalk. This distance can be estimated by using any on-board proximity sensor before stopping.

Using well-known VANET protocols [57], [58], the cars parked along the sidewalk self-organize into a linear vehicular network. In this work, we refer to the resulting network as a *chain* of parked cars. Refer to Fig. 1 for an illustration. By consulting its on-board digital map, each car in the chain determines the width of the street and the speed limit. It also identifies its position in the chain and the pseudonyms of its two adjacent neighbors. When a car is departing or joining the chain, a simple maintenance operation is performed using well-known protocols discussed elsewhere [18] or [58].

It is important to note that since in an on-street parking situation, adjacent parked cars are, typically, a short distance away from each other [59], the tasks inherent to self-organization and maintenance of the chain of parked cars can be performed at low power using a suitable subset of transceivers.

We assume that when ADOPT is booted, there are no pedestrians in the street – pedestrians, if any, are all on the sidewalk. This assumption is non-essential and is made for convenience only. Similarly, we assume that pedestrians step into the street from the sidewalk *in front* of a parked car. If the pedestrians step into the street behind a given parked car, but in front of the next parked car in the chain, the latter will be responsible for undertaking the alerting actions. If there is no car parked behind, then the original parked car will undertake the alerting actions, as described in Section VI, using its rear transceivers instead of the front ones.

Alert messages indicating the presence of a crossing cohort are propagated backward along the chain of parked cars, as illustrated in Fig. 1. As they pass cars in the chain of parked cars, approaching cars will be alerted, using low-power communications, to the reported location (or locations) of crossing pedestrians.

Although not specifically designed with self-driving cars in mind, ADOPT can be easily implemented to run on self-driving cars. When such a car receives an ADOPT “Caution – pedestrian in the street” message, it complies by reducing its

speed without delay using a control system such as the system proposed by [60]. However, at the moment, self-driving cars are not very common, and so ADOPT alerts human drivers by displaying appropriate messages on a dashboard digital map, attempting to minimize distraction. For this purpose, we assume an ADOPT app that is running in approaching cars. The app determines the speed reduction necessary to avoid collision with the crossing cohorts and displays the suggested speed on the dashboard.

#### IV. PEDESTRIAN CLASSIFICATION AND LOCALIZATION

The first task that parked cars need to undertake is to determine if there are pedestrians in the street. If no pedestrians are in the street all is well. Otherwise, the pedestrians have to be accurately localized and their crossing time estimated. Once this information is in hand, approaching cars are alerted to the presence of the crossing cohort. The main goal of this section is to provide the details of pedestrian classification and localization.

##### A. Pedestrian Detection

Recall that, as mentioned in Section III, with each step the pedestrians' shoes generate, for a fraction of a second, an RF signal with a known power  $T$  and a known frequency  $f$  [53]. When a pedestrian walks near a parked car, the transceivers in the car receive the signals generated by the pedestrian's shoes. We calculate the Received Signal Strength  $RSS(Rx)$  at a generic transceiver  $Rx$  using the Free Space propagation model [61]:

$$RSS(Rx) = \frac{T\gamma}{\delta_{Rx}^2}, \quad (1)$$

where  $T$  is the power of the transmitted signal,  $\gamma$  is an environmental constant, and  $\delta_{Rx}$  is the distance between the pedestrian who transmits the signal and the transceiver  $Rx$ .

##### B. Pedestrian Classification

An important task that ADOPT undertakes is the *binary* classification of pedestrians: *on the sidewalk* or *in the street*. We begin by stating and proving a technical result, of an independent interest, that provides a simple criterion for classifying pedestrians.

**Theorem 1** *Consider a pedestrian carrying a transmitter and consider a car parked parallel to the edge of the sidewalk. Assume the car is provided with transceivers,  $L$  and  $R$ , placed at the front corners of the car. Then, the pedestrian is walking parallel to the edge of the sidewalk if, and only if, the difference between the reciprocals of the received signal strengths  $RSS(R)$  and  $RSS(L)$  at  $R$  and  $L$ , respectively, is a constant:*

$$\frac{1}{RSS(L)} - \frac{1}{RSS(R)} = \text{const.} \quad (2)$$

*Proof:* Referring to Fig. 2, consider the horizontal line through the points  $L$  and  $R$  and let  $P$  be the position of the pedestrian. Assume, without loss of generality, that the projection,  $Q$ , of  $P$  onto this line lies to the right of  $R$ . Denote

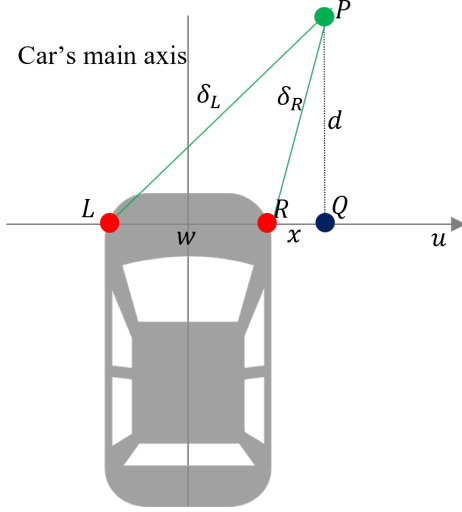


Fig. 2: Illustrating the proof of Theorem 1

by  $d$  the length of the segment  $PQ$ , by  $w$  the length of the segment  $LR$ <sup>3</sup>, and by  $x$  the length of the segment  $RQ$ .

Further, let  $\delta_R$  and  $\delta_L$  be the Euclidean distance between the points  $P$  and  $R$ , and  $P$  and  $L$ , respectively. By applying the Pythagorean theorem to triangles  $LPQ$  and  $RPQ$  we write

$$\begin{cases} \delta_L^2 = (w+x)^2 + d^2 & \text{and} \\ \delta_R^2 = x^2 + d^2 \end{cases}$$

and consequently,

$$\delta_L^2 - \delta_R^2 = (w+x)^2 + d^2 - x^2 - d^2 = w^2 + 2wx. \quad (3)$$

On the other hand,

$$\begin{cases} RSS(R) = \frac{T\gamma}{\delta_R^2} & \text{and} \\ RSS(L) = \frac{T\gamma}{\delta_L^2} \end{cases}$$

implying that

$$\frac{1}{RSS(L)} - \frac{1}{RSS(R)} = \frac{w^2 + 2wx}{T\gamma}. \quad (4)$$

Now, notice that in the right-hand-side of (4),  $w$ ,  $T$  and  $\gamma$  are constants. With this in mind:

- If the pedestrian walks parallel to the edge of the sidewalk then  $x$  remains constant and so the left-hand-side is a constant;
- Conversely, if  $\frac{1}{RSS(L)} - \frac{1}{RSS(R)} = \text{const}$  then, since  $T$ ,  $\gamma$  and  $w$  are constants,  $x$  itself must be a constant and so the pedestrian must walk parallel to the edge of the sidewalk.

This completes the proof of the theorem. ■

**Discussion** Equation (2) establishes a one-to-one correspondence between a subset of real numbers and the set of lines in the plane parallel to the edge of the sidewalk. This is to say, to each line in the plane parallel to the edge of the sidewalk, there corresponds a unique real number and, conversely, to each real number there corresponds exactly one line in the plane parallel to the edge of the sidewalk.

<sup>3</sup>It is useful to think of  $w$  as the width of the car.

By Theorem 1, all the points on the edge of the sidewalk feature the same constant  $c_0$ . Referring, again, to Fig. 2, imagine a transmitter placed at  $Q$ . Here,  $\delta_L = w + z$ ,  $\delta_R = z$  and so, by (4),

$$c_0 = \frac{w^2 + 2wz}{T\gamma}, \quad (5)$$

where, recall,  $z$  is the distance between the car and the sidewalk.

The one-to-one correspondence discussed above is a very useful property because in order to determine if a pedestrian is on the sidewalk, all we have to do is to evaluate the left-hand side of (2) and to compare the result to the value of  $c_0$  from (5). This, in fact, is tantamount to a coarse-grain binary localization of pedestrians: on the sidewalk, or else in the street.

### C. Pedestrian Localization

Pedestrians that are classified as *in the street* have to be localized more accurately, as we are about to explain. Referring to Fig. 3, consider a pedestrian  $P$  and let point  $Q$  be the projection of  $P$  onto the line determined by  $L$  and  $R$ .<sup>4</sup> We assume, without loss of generality, that  $Q$  lies between  $L$  and  $R$ . We assume that the pedestrian crosses the street by walking in a straight line parallel to the front of the parked car (i.e., perpendicular to the sidewalk). Let  $d$  be the length of the line segment  $PQ$  (that is, the vertical distance between the location of the pedestrian and the line  $LR$ ). Further, let  $w$  be the width of the parked car, let  $x$  be the length of the line segment  $QR$ , let  $z$  be the distance from  $R$  to the sidewalk, and write  $y = x + z$ .

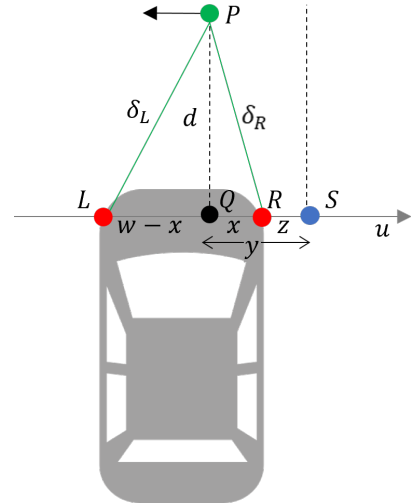


Fig. 3: Illustrating the notation for the proof of Lemma 2.

Now, elementary geometry confirms that  $y$  has the following expression

#### Lemma 2

$$y = \frac{w}{2} + z - \frac{T\gamma}{2w} \left[ \frac{1}{RSS(L)} - \frac{1}{RSS(R)} \right]. \quad (6)$$

<sup>4</sup>It is useful to think of  $L$  and  $R$  as the left and transceivers at the front of the car.

*Proof:*

By using the Pythagorean theorem in the triangles PQL and PRQ we can write:

$$\begin{cases} \delta_L^2 = (w - x)^2 + d^2 & \text{and} \\ \delta_R^2 = x^2 + d^2 \end{cases}$$

and so:

$$\delta_L^2 - \delta_R^2 = (w - x)^2 - x^2 = w^2 - 2wx. \quad (7)$$

From (1),

$$\begin{cases} \delta_L^2 = \frac{T\gamma}{RSS(L)} & \text{and} \\ \delta_R^2 = \frac{T\gamma}{RSS(R)} \end{cases}$$

by plugging these values into (7), we obtain

$$\frac{T\gamma}{RSS(L)} - \frac{T\gamma}{RSS(R)} = w^2 - 2wx.$$

Solving for  $x$  yields

$$\begin{aligned} x &= \frac{w^2}{2w} - \frac{T\gamma}{2w} \left[ \frac{1}{RSS(L)} - \frac{1}{RSS(R)} \right] \\ &= \frac{w}{2} - \frac{T\gamma}{2w} \left[ \frac{1}{RSS(L)} - \frac{1}{RSS(R)} \right] \end{aligned} \quad (8)$$

Finally,

$$\begin{aligned} y &= x + z \\ &= \frac{w}{2} + z - \frac{T\gamma}{2w} \left[ \frac{1}{RSS(L)} - \frac{1}{RSS(R)} \right]. \end{aligned} \quad (9)$$

as claimed.  $\blacksquare$

Now, referring again to Fig. 3, it is clear that since the pedestrians are crossing the street in a direction perpendicular to the sidewalk, in order to specify the location of a crossing pedestrian, it suffices to specify the  $y$  value, as above, along with the value of  $d$ , the vertical distance to the front of the parked car.

In order to determine  $d$ , we compute the area of the triangle PLR in two different ways:

- First, evidently,  $Area(PLR) = \frac{w \cdot d}{2}$ ;
- Second, writing  $p = \frac{\delta_L + \delta_R + w}{2}$ , the same area can be expressed as

$$Area(PLR) = \sqrt{p(p - \delta_R)(p - \delta_L)(p - w)}$$

Consequently,

$$\frac{w \cdot d}{2} = \sqrt{p(p - \delta_R)(p - \delta_L)(p - w)},$$

which, upon solving for  $d$ , yields:

$$d = \frac{2}{w} \sqrt{p(p - \delta_R)(p - \delta_L)(p - w)}. \quad (10)$$

## V. ESTIMATING THE TIME TO CROSS

Recall that a crossing cohort is a group of pedestrians crossing together at the same location. Instead of dealing with each member of the cohort individually, we only concern ourselves with the *tail* of the cohort, defined as the last pedestrian in the cohort. It is clear that if the tail of the cohort has crossed safely, then all pedestrians in the cohort

have crossed safely, too. It is important to note that ADOPT is *privacy-aware* as we are only interested in the location of the tail of the cohort, and not in the actual person that happens to be the last in the cohort.

We now define the tail of a crossing cohort more formally. Recall that the parameter  $y$ , defined in Lemma 2 keeps track of the current distance of a crossing pedestrian to the sidewalk she just departed. Formally, then, at each moment in time, the tail of the crossing cohort is the pedestrian with

$$\min\{y \mid \text{pedestrian classified as in the street}\}. \quad (11)$$

Notice that the tail may change dynamically either because new pedestrians joined the cohort or, simply, because some folks in the cohort walk faster than others. ADOPT updates the tail of the crossing cohort every second.

To manage the tail of a cohort, ADOPT needs to process signals from several pedestrians simultaneously. To accomplish this, the transceivers in the parked car sample frequency  $f$  on which the pedestrians' shoes are transmitting signals,  $m$  times per second. Conceptually, this means that each second is partitioned into  $m$  slots. Assume that each pedestrian takes one step per second, and that each step generates one transmission. For all practical purposes, this transmission occurs, randomly, in one of the  $m$  slots discussed above. Now, suppose that there are  $k$ , ( $k \geq 1$ ), pedestrians in the crossing cohort. We have just set up a "balls-into-bins" model involving  $k$  balls and  $m$  bins. If two or more pedestrians are transmitting in the same time slot, a collision occurs and the outcome cannot be disambiguated.

We are interested to assess the expected number of "clear" transmissions, where one single transmission occurs in a given time slot. For arbitrary  $i$ , ( $1 \leq i \leq k$ ), let  $X_i$  be the indicator random variable that takes on the value 1 if, in a given second, slot  $i$  sees a clear transmission and 0 otherwise. It is easy to see that

$$\Pr[X_i = 1] = \left(1 - \frac{1}{m}\right)^{k-1}$$

and that the expected number,  $E[M]$ , of clear transmissions is

$$\begin{aligned} E[M] &= E[X_1 + X_2 + \dots + X_k] \\ &= E[X_1] + E[X_2] + \dots + E[X_k] \\ &= \Pr[X_1] + \Pr[X_2] + \dots + \Pr[X_k] \\ &= k \left(1 - \frac{1}{m}\right)^{k-1}. \end{aligned}$$

As an illustration, if a given cohort were to contain  $k = 8$  pedestrians, and assuming that frequency  $f$  is sampled 50 times per second, we would expect to see  $E[M] = 8 \times \left(1 - \frac{1}{50}\right)^7 = 8 \times \left(\frac{49}{50}\right)^7 \approx 6.9$  clear transmissions each second.

With this in mind, consider the time ruled into seconds and assume that in second  $t$ , the tail of the current crossing cohort was located at  $y(t)$  and its current speed,  $v(t)$ , has been estimated. The *remaining time to cross* at time  $t$ ,  $\Delta(t)$ , can be estimated as

$$\Delta(t) = \frac{W - y(t)}{v(t)}, \quad (12)$$

where  $W$  is the width of the street that the pedestrians are crossing.



We need to show how these parameters are updated in the next second,  $t + 1$ . We begin by identifying all clear transmissions in second  $t + 1$  and, using equation (11), we obtain the location,  $y(t + 1)$ , of the current tail. We distinguish between the following cases:

**Case 1:**  $y(t) < y(t + 1)$ .

Evidently, in this case, the new tail is closer to the opposite sidewalk. It follows that no new pedestrian has joined the cohort in this second. In this case, it is natural to update the cohort parameters as follows:

- $v(t + 1) = y(t + 1) - y(t)$  m/s;
- $\Delta(t + 1) = \frac{W - y(t + 1)}{v(t + 1)}$ .

**Case 2:**  $y(t) > y(t + 1)$ .

In this case, it is clear that one or more pedestrians have joined the cohort and, consequently, the new tail must be selected from among the pedestrians who have just joined the cohort. There is a complication: we cannot update the speed of the tail, because the tail is new. Instead, we assign to the new tail, tentatively, the average crossing speed. The cohort parameters are updated as follows:

- $v(t + 1) = v_0$ , where  $v_0$  is an estimate of the average pedestrian speed;
- $\Delta(t + 1) = \frac{W - y(t + 1)}{v(t + 1)}$ .

## VI. SAFETY ZONE AND MESSAGE PROPAGATION

ADOPT involves two types of messages, each with its own semantics:

- *Alert messages:* are sent by the parked car that detects a crossing cohort with the intention of establishing a *Safety Zone*, as we are about to describe;
- *Caution messages:* are messages sent by the parked cars in the *Safety Zone* to alert approaching (i.e. moving) cars to the presence of crossing pedestrians.

These two types of messages will be discussed in Subsections VI-A and VI-B, respectively.

### A. Alert messages

Referring to Figure 4, assume, without loss of generality, that car A, the first car in the chain of parked cars, detects a crossing cohort at time  $t$ . Proceeding as discussed in Section V, car A estimates the remaining time,  $\Delta(t)$  (see (12)), it takes the tail of the cohort to cross the street. Using this information, car A determines the distance,  $D(t)$ , the alert messages will have to be propagated along the chain as follows:

$$D(t) = [\Delta(t) + r] \cdot v_{max}, \quad (13)$$

where  $r$  is the *driver reaction time*, estimated to be between 1.24 seconds and 2 seconds [62]. If self-driving cars are considered, then  $r$  is set to zero, since the driver reaction time is a human factor and does not affect self-driving cars. Finally, car A propagates the alert message containing: its own location,  $x(A)$ , on the digital map, the current time,  $t$ , and the Distance-to-Live  $D(t)$  of the alert message in meters.

Referring to Fig. 4 again, the area of length  $D(t)$ , defined in (13), starting at car A and running down the chain of parked

cars is called the *Safety Zone* associated with the crossing cohort detected by car A. Each parked car in the chain of parked cars, upon receiving the alert message originated by car A, compares its own location with that of A and determines if the distance from A is smaller than or equal to  $D(t)$ . If so, it marks itself as being in the *Safety Zone* and propagates the alert message further along the chain.

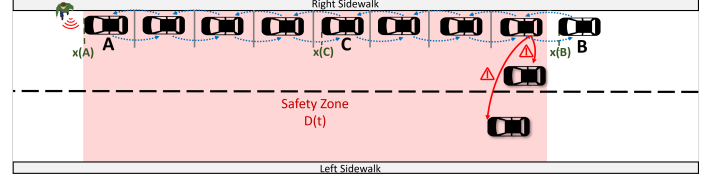


Fig. 4: *Parked cars in the Safety Zone propagate alert messages within the estimated propagation distance to alert approaching cars.*

As an illustration, in Fig. 4, assume that car C has just received the alert message from the previous car in the chain. Let  $x(A)$  and  $x(C)$  be the x-coordinates of A and C, respectively. If  $|x(A) - x(C)| \leq D(t)$  then C remembers that it belongs to the *Safety Zone* and propagates the message further down the chain. Continuing in this way, the alert message will reach, eventually, car B. When car B receives the alert message, it finds that  $|x(A) - x(B)| > D(t)$ , and so it discards the message. As illustrated in Fig. 4, car B is not in the *Safety Zone*.

### B. Caution messages

Each parked car inside the *Safety Zone* is tasked with broadcasting a “Caution – pedestrians in the street” (Caution, for short) message to approaching cars. This broadcast must be done at low power, as passing cars are a short distance away from parked cars. The Caution message contains:

- the location  $x(A) + d$  of the crossing cohort, where  $d$  was computed in (10);
- the time,  $t + \Delta(t)$ , at which the cohort is expected to have crossed the street.

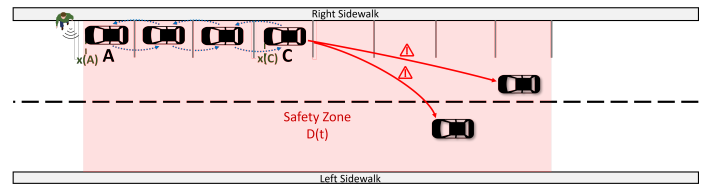


Fig. 5: *The Last car in the chain delivers the Caution message to the approaching car via DSRC if the chain length is less than  $D(t)$ .*

In the unlikely event where many cars in the chain of parked cars depart, leaving big gaps in the chain, as shown in Fig. 5, the last car in the chain uses its DSRC transmitter to broadcast the Caution message to inform approaching cars of the location of the crossing cohort. As illustrated in Fig. 5, car C with  $|x(A) - x(C)| < D(t)$  does not detect any car behind it.

Hence, car C will use its DSRC transmitter to broadcast the "Caution" message at a distance of  $D(t) - x(C)$ , where  $x(C)$  is the location of C.

In the next second,  $t + 1$ , a new estimate  $D(t + 1)$  is made as discussed in Section V. If  $D(t + 1) > D(t)$  then an updated alert message is sent with Distance-to-Live  $D(t + 1)$ . Otherwise, no action is needed.

## VII. HOW APPROACHING CARS DETERMINE A SAFE SPEED

The main goal of this section is to show how approaching cars, alerted to the presence of crossing cohorts, adjust their speed in such a way that they avoid colliding with the crossing pedestrians.

Our approach is novel and is based of a new way of looking at the time-space diagram (see the Appendix for a refresher).

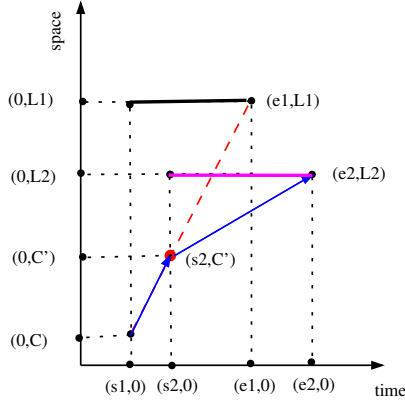


Fig. 6: Illustrating the computation of the safe average speed in the case of two crossing cohorts.

Referring to Fig. 6, consider a car moving North-bound along a street. At time  $s1$ , the car receives a "Caution – pedestrians in the street" message alerting it to a crossing cohort at location  $(0, L1)$ . Assume that the location of the car at time  $s1$  is  $(s1, C)$  and that the cohort will finish crossing the street at time  $e1$ .

Proceeding as indicated in Subsection B of the Appendix, the approaching car computes the maximum safe speed:

$$v_{safe} = \min \left\{ v_{max}, \frac{L1 - C}{e1 - s1} \right\}, \quad (14)$$

where  $v_{max}$  is the speed limit along the street.

Traveling at this safe speed North-bound, the approaching car receives, at time  $s2$ , a second "Caution – pedestrians in the street" message alerting it to the presence of a second crossing cohort. This cohort crosses the street at location  $(0, L2)$  and will finish crossing at time  $e2$ . How should the car change its speed to avoid an accident?

In order to answer this question, the first task is to determine the location,  $(s2, C')$  of the car at time  $s2$ . This can be done by noting that  $v_{safe}$  in equation (14) can be written as

$$\frac{L1 - C}{e1 - s1} = \frac{C' - C}{e1 - s1}.$$

Solving for  $C'$  yields:

$$C' = C + \frac{(L1 - C)(s2 - s1)}{e1 - s1}.$$

With  $C'$  firmly in hand, the car updates the current safe speed  $v_{safe}$  in (14) as follows:

$$\begin{aligned} v_{safe} &= \min \left\{ v_{safe}, \frac{L2 - C'}{e2 - s2} \right\} \\ &= \min \left\{ v_{max}, \frac{L1 - C}{e1 - s1}, \frac{L2 - C'}{e2 - s2} \right\}. \end{aligned} \quad (15)$$

The justification of (15) is simple. The car needs to select the largest average safe speed and this is the smallest of the slopes of the lines segments determined by the points  $(s2, C')$  and  $(e1, L1)$  on the one hand, and the points  $(s2, C')$  and  $(e2, L2)$  on the other.

At time  $e1$ , the car realizes that the first cohort has finished crossing the street and will adjust its speed again:

$$v_{safe} = \min \left\{ v_{max}, \frac{L2 - C'}{e2 - s2} \right\}. \quad (16)$$

In Fig. 6,

$$\min \left\{ v_{max}, \frac{L2 - C'}{e2 - s2} \right\} = \min \left\{ v_{max}, \frac{L1 - C}{e1 - s1}, \frac{L2 - C'}{e2 - s2} \right\},$$

and, consequently, the car continues driving at the same speed.

Next, at time  $e2$ , the car realizes that the second cohort has finished crossing and so it will adjust its speed again:

$$v_{safe} = \min \{ v_{max} \} = v_{max}, \quad (17)$$

essentially, reverting to the maximum allowed speed.

The same procedure is then continued, exactly as described, should other "Caution – pedestrians in the street" be received by the car in the future.

## VIII. SIMULATION MODEL

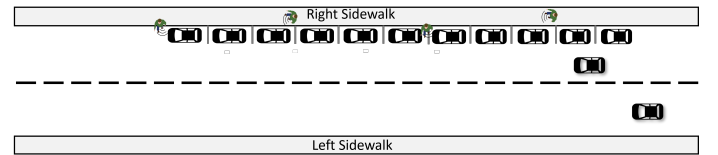


Fig. 7: An instance of the ADOPT simulation model.

We validated the theoretical findings of ADOPT by testing them on simulated traffic data. For this purpose, we used SUMO (Simulation of Urban MObility) [63] to generate pedestrian and car traffic data for the ADOPT simulation model illustrated in Fig. 7.

Our simulation model consists of a *one-way* street with a road-side parking lane on the right side of the street and sidewalks on both sides. Approaching cars enter at the end of the street and exit from the opposite end. In our simulation model, the pedestrians are not restricted to crossing at intersections but, indeed, they may cross *midblock* a prevalent behavior [15].

For the reader's convenience, we summarize the simulation parameters in Table I.



TABLE I: A summary of simulation parameters

Parameter	Value
RF signal frequency $f$	2.4 GHz
Transmission Power $T$	2 mW
Street width $W$	12.8 m
Distance from R transceiver to the sidewalk $z$	0.4 m
Number of detected pedestrians/sec $[\mu, \sigma]$	[1.8, 1.4]
Pedestrians speeds $[\mu, \sigma]$	[1.15, 0.13] m/sec
Average speed $v_0$	1.2 m/sec
Number of crossing pedestrians/sec $[\mu, \sigma]$	[0.11, 0.32]
Street speed limit $v_{max}$	15 m/sec
Simulation step length	1 sec
Simulation steps	3600 sec (1 hour)

The data we collected from SUMO are as follows: street and sidewalk dimensions, pedestrians' locations, pedestrians' speeds, parked cars' locations and dimensions, and approaching cars' speed and location at each time step. Data collected from SUMO is our ground truth, i.e., "actual", information about pedestrians and cars traffic.

We modeled pedestrians' radio signals by setting a constant transmission power equal to 2 mW transmitted from their actual locations. We then obtained the actual Euclidean distances  $\delta_{Rx}$  between the pedestrian locations and the four transceivers located at the four corners of cars.

#### A. Modeling RSS Noise

In real-life situations, the Received Signal Strength ( $RSS$ ) measurements experience random variations due to hardware-based parameters such as thermal noise, or due to the natural behavior of the signal as it is reflected by the ground [64]. Being close to the ground, we assume that there are no obstacles between the pedestrians' shoes and the transceivers.

We modeled the uncertainty in the  $RSS$  produced by receiving either more or less power than the original  $RSS$  as a Gaussian random variable  $\Phi_\sigma$  with zero mean and a standard deviation  $\sigma$  as follows:

$$RSS'(Rx) = RSS(Rx) + \Phi_\sigma,$$

where  $RSS'$  is the noisy received signal strength at a generic transceiver  $Rx$ . We set  $\sigma$  to 0.3 mW since we only consider short transmission ranges and near-the-ground communication. The added noise affects the distance we estimate based on the  $RSS$ . We measured the impact of noise by calculating the absolute error  $\xi$  of the estimated distance at each transceiver  $RSS(R)$  and  $RSS(L)$  where  $\xi_{\delta_R} = |\hat{\delta}_R - \delta_R|$  and  $\xi_{\delta_L} = |\hat{\delta}_L - \delta_L|$ . Fig. 8 shows the distribution of the absolute errors in distance estimated from  $RSS'(R)$  and  $RSS'(L)$  plotted against the actual distances (a)  $\delta_R$  and (a)  $\delta_L$  obtained from SUMO respectively. Note that the errors shown are observed at every 0.2-meters window. Results showed that the added noise causes minor distance estimation errors in ranges near the transceivers, but the errors increase as the pedestrians move away from the transceivers.

As the noise affects the  $RSS$  at both transceivers, it also affects the result of (4). Consequently, the noise impacts the one-to-one mapping, discussed in Section IV, between the set

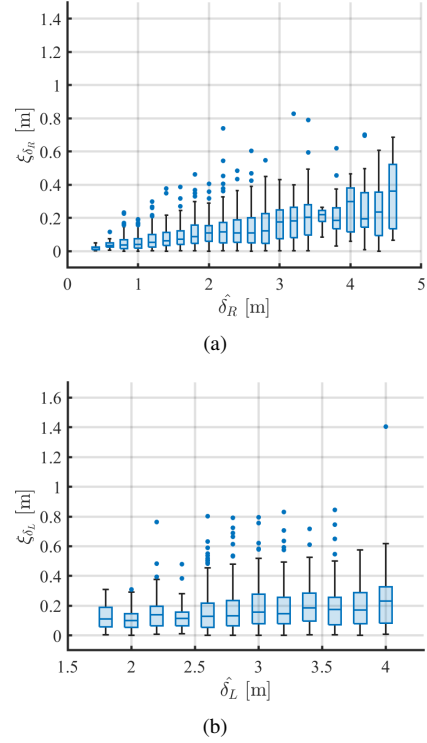


Fig. 8: Absolute error of estimated distances  $\delta_R$  and  $\delta_L$  against the actual distances (a)  $\delta_R$  and (b)  $\delta_L$ .

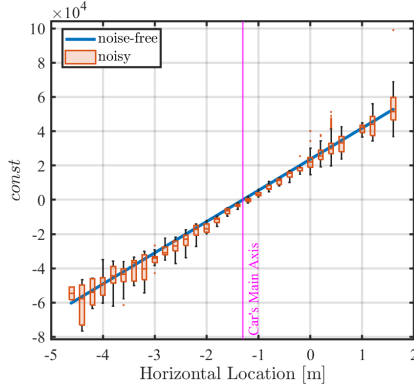
of lines parallel to the edge of the sidewalk and the  $const$  values as each line will have many  $const$  values. To determine the range of inaccuracy in  $const$ , we define a 0.2-meters window of the horizontal position before and after the sidewalk and aggregate the calculated noisy  $const$  from  $RSS'(L)$  and  $RSS'(R)$  at each window as we show in Fig. 9(a). To compare the noisy  $const$  with the noise-free  $const$ , we show in the same figure the noise-free  $const$ . The results showed that the noise impacts the  $const$  if pedestrians are far from the main axis of the car (i.e. middle of the LR line segment), while it has a lower impact near the LR midpoint the pedestrians are close to both transceivers and  $const$  is almost zero. This affected also the classification based on the threshold  $c_0$ . Referring to Fig. 9(b), all  $const$  values of pedestrians walking on sidewalk are greater than  $c_0$ . Similarly, all  $const$  values of pedestrians who are in the street are less than  $c_0$ . However, with the noisy  $const$ , several  $const$  values of pedestrians walking on the sidewalk are less than  $c_0$ , and several  $const$  values of pedestrians walking in the street are greater than  $c_0$ .

## IX. EVALUATION

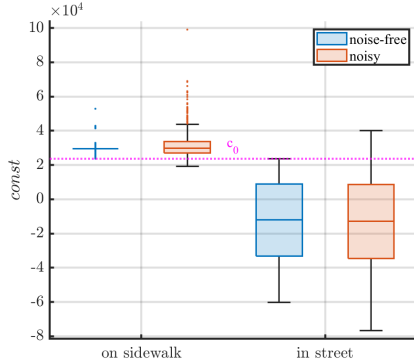
We evaluated the performance of ADOPT in two scenarios:

- **Scenario 1 – Noise-free mode:** in which we performed pedestrian classification and crossing time estimation using the actual data generated by SUMO;
- **Scenario 2 – Noisy mode:** in which we performed pedestrian classification and crossing time estimation using noisy RSS to have a more realistic evaluation.

We demonstrate the performance of ADOPT in both scenarios above. Specifically, in Subsection IX-A we discuss the



(a) The noise produces multiple  $const$  values for the same parallel line to the sidewalk while the actual  $const$  is unique for each line.



(b) Distribution of  $const$  of pedestrians' signals per pedestrian's class (on the sidewalk and in the street).  $c_0$  is used as a threshold to classify pedestrians.

Fig. 9: Effect of noise on  $const$

accuracy of pedestrian classification; in Subsection IX-B we discuss the accuracy of pedestrian localization, once they are in the street; the accuracy of pedestrian street traversal speed is discussed in Subsection IX-C; the accuracy of the remaining crossing time is discussed in Subsection IX-D; the accuracy of establishing the Safety Zone is discussed in Subsection IX-E. Finally, Subsection IX-F offers an end-to-end evaluation of ADOPT.

#### A. Accuracy of pedestrian classification

We evaluated the accuracy of pedestrian classification as *on the sidewalk* or *in the street* by using the following formula

$$accuracy = \frac{TP + TN}{TP + TN + FP + FN} \times 100, \quad (18)$$

where

- TP (True Positive): is the total number of pedestrians that were correctly identified to be in the street;
- TN (True Negative): is the total number of pedestrians that were correctly identified to be on the sidewalk;
- FP (False Positive): is the total number of pedestrians incorrectly classified as in the street; and,
- FN (False Negative): is the total number of pedestrians incorrectly identified as on the sidewalk.

We obtained the ground truth of pedestrians classes directly from SUMO generated data. Referring to Table II the accuracy of pedestrian classification in the noise-free mode is 100% accuracy, while the accuracy dropped to 93.25% in the noisy mode.

To investigate the impact of noise on the classification performance in noisy mode, in Fig. 10 we plot the classification accuracy against the horizontal location of the transmitted signal from the edge of the sidewalk that is indicated with value 0. Locations with negative values are in the street while locations with positive values are on the sidewalk. We noticed that the classification accuracy only drops when the transmitted signal is within few decimeters away from the edge of the sidewalk (i.e. location 0).

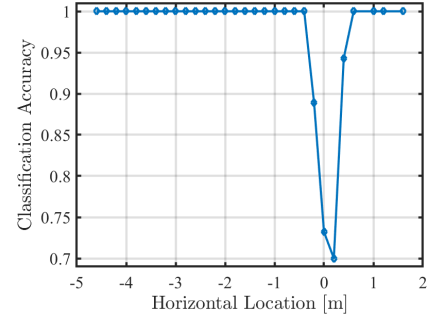


Fig. 10: Aggregated classification accuracy at horizontal locations before and after the edge of the sidewalk.

To better understand what is going on, we investigated the accuracy metrics TP, FP, TN, FN, defined above in more detail. Referring to Fig. 11(a), the accuracy drops when we have FP and FN due to the noisy  $const$  (denoted by  $const'$ ). We noticed that FP classification occurs if  $const$  is less than  $c_0$  and, at the same time,  $const'$  is greater than  $c_0$ . This means we have FPs if the noise generates  $const$  above the threshold  $c_0$  while the actual  $const$  is lower than the threshold. Similarly, FN classifications occur if  $const$  is greater than  $c_0$  and, at the same time,  $const'$  is less than  $c_0$ . This means we have FN if the noise generated  $const'$  below the threshold  $c_0$  while the actual  $const$  is above the threshold. From the figure, we can see that this happens only in a limited area around  $c_0$ . To translate this to spatial data, in Fig. 11(b) we plotted  $const'$  corresponding to the horizontal location of the transmitted signal.

Obviously, high FN puts pedestrians at the risk as they enter the street and ADOPT does not alert the approaching cars. On the other hand, high FP results in flooding the approaching vehicles with incorrect alert messages while the pedestrians are on the sidewalk. To assess where ADOPT has misclassification, we define our metric False Positive Per Location FPPL and False Negative Per Location FNPL where FPPL is the percentage of FP per horizontal location aggregated at each 0.2 meters, and FNPL is the percentage of FN per horizontal location aggregated at each 0.2 meters as well. Fig. 11(c) shows that FNPL is high only at locations situated a few decimeters away from the edge of the sidewalk. Moreover, ADOPT has higher FPPL a few decimeters away from the edge of the sidewalk. In conclusion, the ADOPT pedestrian

TABLE II: Overall Accuracy of Pedestrian Classification

Actual Class		Predicted Class (noise-free mode)		Predicted Class (noisy mode)	
		in street (positive)	on sidewalk (negative)	in street (positive)	on sidewalk (negative)
	in street (positive) on sidewalk (negative)	340 (TP) 0 (FP)	0 (FN) 1216 (TN)	316 (TP) 81 (FP)	24 (FN) 1135 (TN)
Accuracy		100%		93.25%	

TABLE III: ADOPT Estimation RMSE

RMSE	noise-free mode	noisy mode
$E_y$	0.00 m	0.26 m
$E_d$	0.00 m	0.24 m
$E_v$	0.05 m/sec	0.11 m/sec
$E_\Delta$	0.51 sec	1.21 sec
$E_D$	12.79 m	42.23 m

classification scheme is able to classify pedestrians accurately even in the presence of noisy signals.

The other metrics we use to evaluate empirically the performance of ADOPT are: the accuracy of pedestrian localization, the accuracy of crossing time estimation, the accuracy of the remaining crossing time, as well as the accuracy of the Safety Zone size. We use Root Mean Squared Error (RMSE) to measure the accuracy of these estimations. We show the overall result of the RMSE in Table III. In the following subsections, we discuss each of them in detail.

### B. Accuracy of pedestrian localization

To measure the overall accuracy of pedestrian localization, we evaluated  $E_d$  and  $E_y$ , where  $E_d$  is the RMSE of location of pedestrians in front of the parked car (the vertical distance of the pedestrian) and  $E_y$  is the RMSE in estimating the pedestrian's distance from the edge of the sidewalk (the horizontal distance of crossing pedestrians) as follows:

We evaluated  $E_d$  as follows:

$$E_d = \sqrt{\frac{\sum_{j=1}^M (\hat{d}_j - d_j)^2}{M}}$$

where  $M$  is the total number of received signals and  $\hat{d}_j$  and  $d_j$  are, respectively, the actual and estimated vertical distances of the received signal.

Similarly, we calculate:

$$E_y = \sqrt{\frac{\sum_{j=1}^{M_s} (\hat{y}_j - y_j)^2}{M_s}}$$

where  $M_s$  is the total number of received signals that are actually detected in the street.  $\hat{y}_j$  and  $y_j$  are the actual and estimated horizontal distances. Recall that  $y$  is only calculated when a pedestrian is classified as in the street.

To show the result in detail, we determined a 0.2-meters window of  $\hat{d}$ . Fig. 12(a) shows that the aggregated absolute error  $\xi_d = |\hat{d} - d|$  is zero in the noise-free mode and does not exceeds 1.5 meters in the noisy mode.

Similarly, we determined a 0.2-meters window of  $\hat{y}$  to observe the absolute error at each window. The absolute error

of  $y$  is  $\xi_y = |\hat{y} - y|$ . Fig. 12(b) shows that the estimation of  $y$  in the noise-free mode is accurate since we have zero aggregated error. However, the aggregated error increases in noisy mode. The errors are lower as pedestrians start crossing the street because they are closer to the main axis of the car (i.e. around  $y = 1.3$ ) and the noise is low in this area as we showed previously in Fig. 9(a).

### C. Accuracy of crossing speed estimation

We used RMSE to measure the overall accuracy of estimating the pedestrian's speed  $v$  as follows:

$$E_v = \sqrt{\frac{\sum_{i=1}^N (\hat{v}_i - v_i)^2}{N}}$$

where  $N$  is the total number of pedestrians generated in the simulation, and  $\hat{v}_i$  and  $v_i$  are, respectively, the actual and the estimated speed of each pedestrian who was actually in the street. We chose to average the speed of each pedestrian individually because one pedestrian may vary her speed in SUMO. Fig. 13(a) shows the Empirical Distribution Cumulative Function ECDF of the actual speeds, that are retrieved from SUMO, and the speeds that we estimate in noise-free and lastly the speed estimate in the noisy mode. The results showed that the noise affects the speed estimation as we can see from the difference between the actual and the noisy estimates in the figure. In addition, we noticed that the difference between the actual and noise-free estimates is due to the change of the crossing cohort size, and this happens only when a new pedestrian joins the cohort. We show in Fig. 13(b) the ECDF after removing the samples where a new pedestrian joins the cohort. As it can be seen in the figure, the difference between the noise-free estimated speed and the actual speed is lower when the cohort size is fixed.

### D. Accuracy of the remaining crossing time

We used the same RMSE formula to measure the accuracy of the remaining crossing time:

$$E_\Delta = \sqrt{\frac{\sum_{i=1}^N (\hat{\Delta}_i - \Delta_i)^2}{N}}$$

where  $\hat{\Delta}_i$  and  $\Delta_i$  are, respectively, the actual and estimated remaining time to cross for each pedestrian. Fig. 14(a) shows the ECDF of the average crossing time for each pedestrian in the street. We calculated the actual remaining crossing time based on the actual speed retrieved from SUMO. As the noise affects the speed, it also affects the remaining crossing time as we show in the figure. We noticed also that the difference

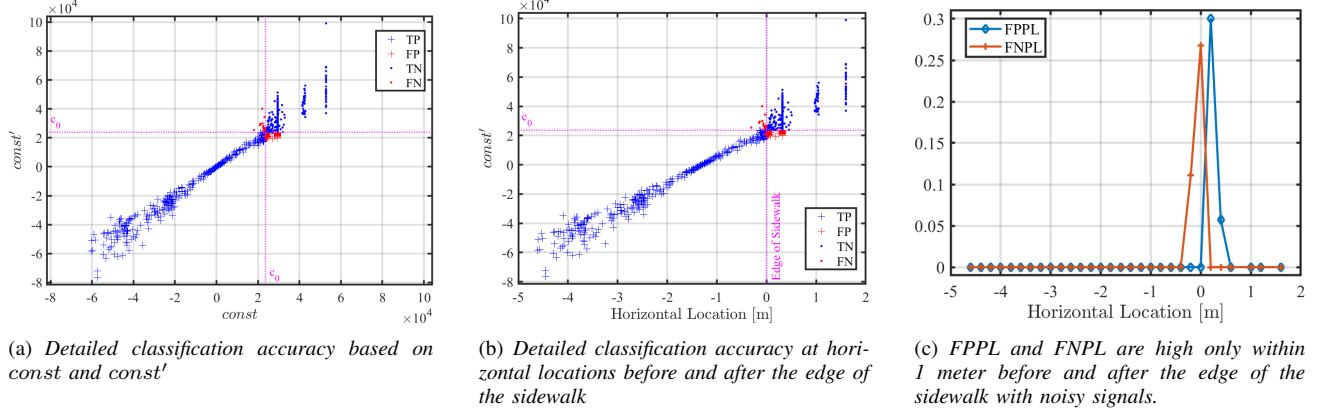


Fig. 11: ADOPT performance in pedestrian classification

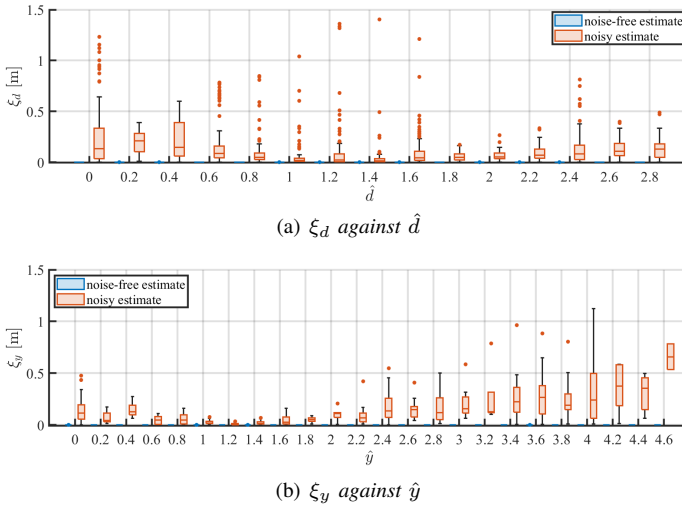


Fig. 12: Distribution of localization error against the actual location

between the actual and noise-free estimation is due to the change of the crossing cohort size, and this happens only the first time a new signal is detected in the crossing cohort. We show in Fig. 14(b) the ECDF after removing the samples where a new pedestrian joins the cohort. As it can be seen from the figure, the difference between the noise-free estimate and the actual time to cross is lower.

#### E. Accuracy of Safety Zone size

The RMSE of estimating the Safety Zone size, which is determined by the propagation distance  $D(t)$ , for each pedestrian is calculated as follows:

$$E_D = \sqrt{\frac{\sum_{i=1}^N (\hat{D}_i - D_i)^2}{N}}$$

where  $\hat{D}_i$  and  $D_i$  are, respectively, the actual and estimated propagation distances.  $\hat{D}_i$  is calculated based on the actual remaining time to cross  $\hat{\Delta}_i$ . Fig. 15 shows the ECDF for the propagation distance estimation averaged for each pedestrian

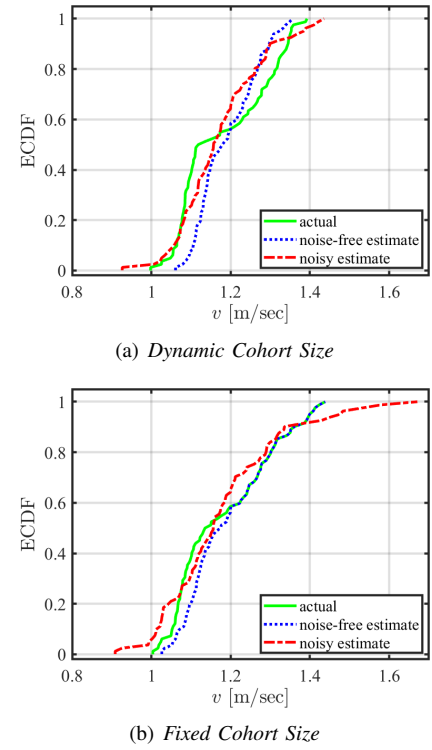
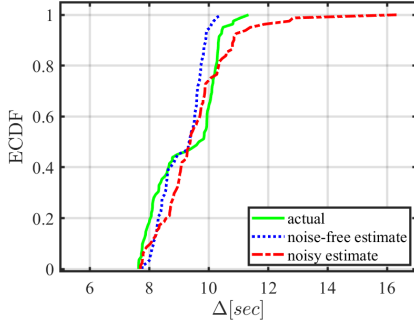


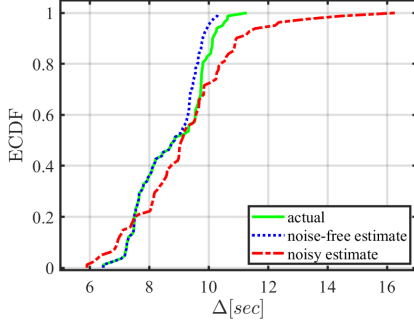
Fig. 13: ECDF of Pedestrian Speeds

in the dynamic and fixed cohort sizes. We noticed that the difference between the actual and the noise-free estimate is less in the fixed cohort size. The difference between them increases based on the error of  $\Delta$  estimation.

To justify the difference between the actual and estimated propagation distance, we measured the relative error of estimating  $\Delta$  and  $D$  in noise-free mode for fixed size cohort compared to their actual values where the *relative error* =  $\text{actual value} - \text{estimated value}$ . The results showed that there is a high correlation between the relative error of estimating  $\Delta$  and  $D$  as we show in Fig. 16. The figure also shows that the majority of  $\Delta$  errors are less than 3 seconds and cause about additional 40 meters of  $D$ . We see a high



(a) Dynamic cohort size



(b) Fixed cohort size

Fig. 14: ECDF of remaining crossing time

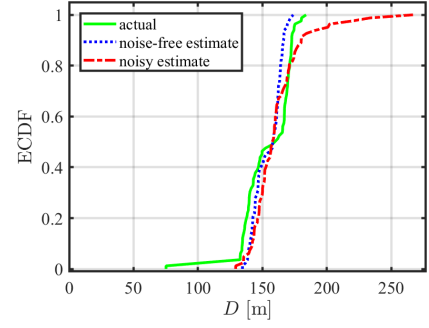
error in  $D$  since each  $\pm 1$  second of error in  $\Delta$  is multiplied by the car's speed and the added  $r$ , so this second produces about  $\pm 15$  meters of  $D$  error. If the error is positive then ADOPT estimates a larger safety zone and the pedestrian is safe. Indeed, the risk may increase if the estimation is less than needed.

In conclusion, the ADOPT classification accuracy depends on the amount of RSS noise that affects the  $const$  values near the edge of the sidewalk. For localization, the accuracy of ADOPT depends on the RSS noise and the distance of the pedestrian from the transceiver receiving the strongest signals. ADOPT accuracy in estimating the speed, remaining crossing time and Safety Zone size depends on the noise and changes in cohort size.

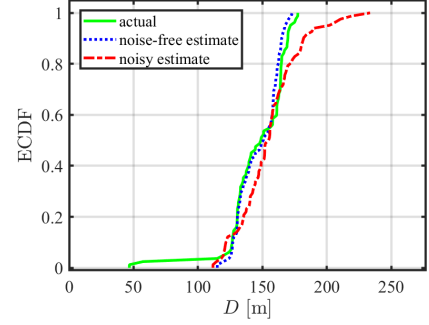
#### F. Evaluation of occluded pedestrian protection

To evaluate the performance of ADOPT as an end-to-end system to protect occluded crossing pedestrians, we calculated the speed of the approaching car upon reaching the pedestrian crossing area. We assumed that the driver or the automated vehicle react to the "Caution" message promptly upon receiving it from the ADOPT app running in the car. Note that SUMO has implemented a collision avoidance model to force vehicles to reduce their speed if there are crossing pedestrians. We disabled this mode before we generated the vehicular traffic.

Referring to Fig. 17, the approaching cars generated in SUMO adopt the new speed  $v_{safe}$  upon receiving the "Caution" messages as they approach the crossing pedestrians. We observed and aggregated the speeds at every 13-meters of car-to-pedestrians distances. As it can be seen also in the

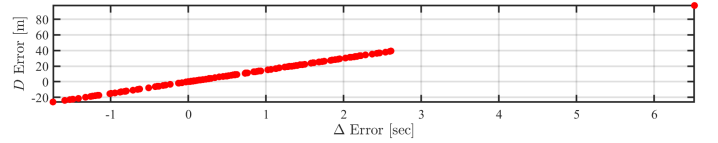


(a) Dynamic cohort size



(b) Fixed cohort size

Fig. 15: ECDF of propagation distance.

Fig. 16: Correlation between the estimation error of  $D$  and  $\Delta$ 

figure, the cars start maintaining their safe speeds gradually while they are approaching the crossing pedestrians which allows a smooth speed reduction without the need for a sudden stop. To compare the speed reduction caused by ADOPT with the speed of cars without ADOPT, we plotted their cruising speeds  $v_{cruising}$  from SUMO in the same figure. We called it  $v_{cruising}$  since SUMO cars do not maintain a fixed speed while moving, and also each car has its own speed random distribution with a determined maximum speed equal to the street's speed limit  $v_{max}$ .

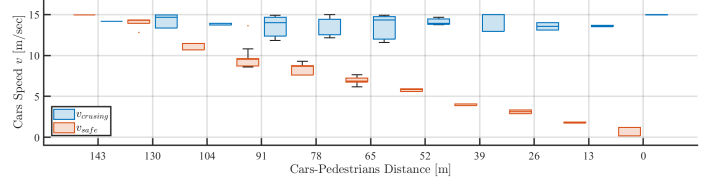


Fig. 17: All approaching cars maintained safe speeds upon receiving the "Caution" message from ADOPT while they keep their cruising speeds without ADOPT "Caution" messages.

In the following, we show some examples from the simulation of approaching cars receiving ADOPT "Caution" message and changing their speed accordingly:

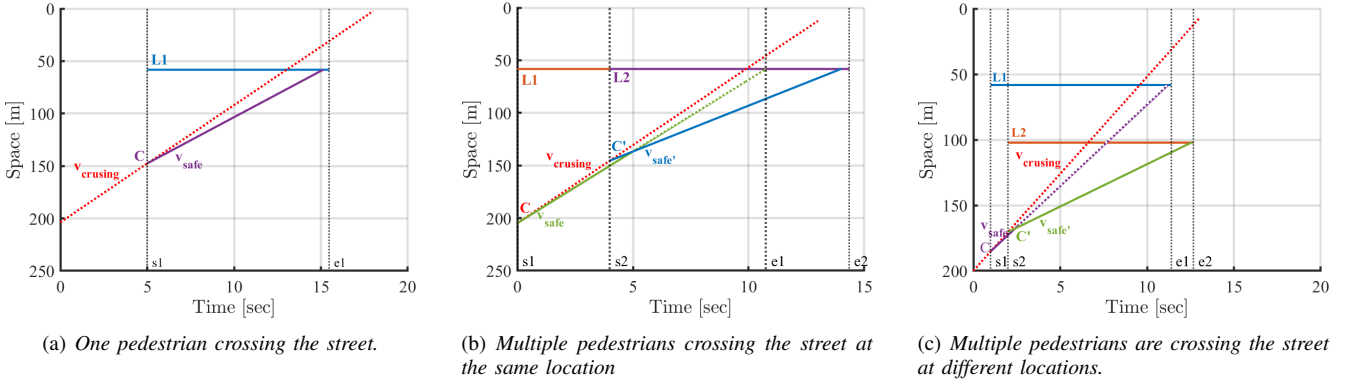


Fig. 18: Moving vehicle reduces its speed upon receiving "Caution" message from ADOPT in many cases.

In Fig. 18(a), the approaching car with speed  $v_{max}$  receives a "Caution" message at location  $C$  and time  $s1$  for a pedestrian crossing at location  $L1$ . The car reduces its speed to  $v_{safe}$  as a response to the alert message. We noticed that the car may intersect slightly before  $(L1, e1)$  due to the error in estimating  $d$  and the crossing time  $\Delta$ . In another example Fig. 18(b), the car receives another "Caution" message at location  $C'$  as a new pedestrian joins the cohort from the same location of  $L$ , and finishes crossing at  $e2 > e1$ . In this case, the car finds that the new speed (denoted by  $v_{safe'}$ ) is lower than  $v_{safe}$ , so it adopts the new speed  $v_{safe'}$  to avoid the collision. The expected reaction of the approaching car is to reduce its speed because the crossing time now becomes longer as a new pedestrian joins the cohort.

In a more complex example, cars report pedestrians at different locations  $L1$  and  $L2$  as in Fig. 18(c). When the car receives a new "Caution" message at time  $s2$  and location  $C'$ , it calculates the new speed and finds that it is less than its current speed because  $L2$  is closer than  $L1$ . Thus, it adopts the new speed  $v_{safe'}$  until the pedestrian finish crossing.

In conclusion, approaching cars were able to maintain low speeds to avoid collision with the occluded crossing pedestrian accurately and in a timely manner based on the "Caution" messages received from ADOPT. This proves that ADOPT works end-to-end to effectively protect crossing pedestrians.

## X. CONCLUDING REMARKS AND FUTURE WORK

The common philosophy of all the pedestrian detection approaches of which we are aware is that this task should be undertaken by the moving cars themselves. In sharp departure from this philosophy, we proposed to employ cars parked along the sidewalk to detect and protect crossing pedestrians.

In support of this goal, we have proposed ADOPT: a system for Alerting Drivers to Occluded Pedestrian Traffic. ADOPT lays the theoretical foundations of a system that uses the on-board resources of parked cars to:

- Detect the presence of a group of crossing pedestrians – a crossing cohort;
- Predict the time the last member of the cohort takes to cross the street;

- Send alert messages to those approaching cars that may reach the crossing area while pedestrians are still in the street;
- Show how approaching cars can adjust their speed to avoid crashing into crossing pedestrians.

Importantly, in ADOPT all communications occur over very short distances and at very low power. Our extensive simulations using SUMO-generated pedestrian and car traffic, have shown the effectiveness of ADOPT in detecting and protecting crossing pedestrians.

In spite of this, there are a number of topics that need more work. First, the problem of information overload has to be mitigated. The problem arises when the (human) driver of an approaching car is alerted to the presence of various crossing cohorts. We are planning to design an app that minimized the information overload and, consequently, driver distraction.

Second, it is of interest to optimize the process of disseminating alert messages as a function of the residual crossing time. In the current version of the paper "All clear" messages informing approaching cars that the cohort has finished crossing are not used. Incorporating them into ADOPT is targeted for future work.

Third, security and privacy are very important and are getting active attention as discussed in the next subsection.

### A. Security and Privacy in ADOPT

ADOPT involves two types of wireless communications: V2P and V2V. In the following, we discuss the security aspects of our communication types.

- Pedestrian to parked vehicle communications: In the pedestrian detection and localization process, the system reads transmitted signals and makes decisions based solely on the signal strength and not on the identity of the pedestrians. These decisions are based on anonymous received signal strengths that do not require unique identifiers. Also, ADOPT detects and localizes pedestrians in short-range communications that do not require transmitting the pedestrians' private data. With the proposed mechanism of pedestrian localization, ADOPT preserves pedestrians' privacy and security. In spite of this, we may consider a potential attack that may be mounted against



ADOPT such as a Denial of Service (DoS) attack. In this attack, a group of pedestrians may stomp their feet on the ground to activate the system. Our approach to pedestrian classification can distinguish if the signal is coming from the sidewalk or the street. If this group of people is generating signals from the street, they are at risk and the system should notify approaching cars regardless of their intent.

- **Parked vehicle to approaching vehicle communication:** This type of communication involves the known security threats in V2V communications [65]. However, the short-range communication used in our system should allow the use of frequency hopping [66] to prevent attackers from sniffing or injecting fake information into V2V network. Moreover, short-range V2V communications have their security advantages [11] that are not present in long-range V2V communications. It is of great interest to develop security primitive that leverage the type of short-range communications that are used throughout the system [67], [68], [69].

## REFERENCES

- [1] GHSA, "Pedestrian Traffic Fatalities by State: 2021 Preliminary Data," <https://www.ghsa.org/resources/Pedestrians22>, June 2021.
- [2] L. Yue, M. Abdel-Aty, Y. Wu, O. Zheng, and J. Yuan, "In-depth approach for identifying crash causation patterns and its implications for pedestrian crash prevention," *J. Safety Res.*, vol. 73, pp. 119–132, Jun. 2020.
- [3] I. Mahdinia, A. J. Khattak, and A. Mohsena Haque, "How effective are pedestrian crash prevention systems in improving pedestrian safety? harnessing large-scale experimental data," *Accid. Anal. Prev.*, vol. 171, p. 106669, Jun. 2022. [Online]. Available: <http://dx.doi.org/10.1016/j.aap.2022.106669>
- [4] S. El Hamdani, N. Benamar, and M. Younis, "Pedestrian support in intelligent transportation systems: Challenges, solutions and open issues," *Transp. Res. Part C: Emerg. Technol.*, vol. 121, p. 102856, Dec. 2020. [Online]. Available: <https://www.sciencedirect.com/science/article/pii/S0968090X20307567>
- [5] S. Gilroy, E. Jones, and M. Glavin, "Overcoming occlusion in the automotive environment—a review," *IEEE Trans. Intell. Transp. Syst.*, vol. 22, no. 1, pp. 23–35, 2019.
- [6] C. Ning, L. Menglu, Y. Hao, S. Xueping, and L. Yunhong, "Survey of pedestrian detection with occlusion," *Complex & Intelligent Systems*, vol. 7, no. 1, pp. 577–587, Feb. 2021.
- [7] S. Zhang, R. Benenson, M. Omran, J. Hosang, and B. Schiele, "How far are we from solving pedestrian detection?" in *Proceedings of the IEEE conference on computer vision and pattern recognition*, 2016, pp. 1259–1267.
- [8] P. Sun and A. Boukerche, "Challenges and potential solutions for designing a practical pedestrian detection framework for supporting autonomous driving," in *Proc. 18th ACM Symposium on Mobility Management and Wireless Access (MobiWac'20)*, Nov. 2020, pp. 75–82.
- [9] T. S. Combs, L. S. Sandt, M. P. Clamann, and N. C. McDonald, "Automated vehicles and pedestrian safety: Exploring the promise and limits of pedestrian detection," *Am. J. Prev. Med.*, vol. 56, no. 1, pp. 1–7, Jan. 2019.
- [10] T. Combs, L. Sandt, M. Clamann, and N. McDonald, "Automated vehicles and pedestrian safety: exploring the promise and limits of pedestrian detection," *American journal of preventive medicine*, vol. 56, no. 1, pp. 1–7, 2019.
- [11] D. B. Rawat, B. B. Bista, G. Yan, and S. Olariu, "Vehicle-to-Vehicle connectivity and communication framework for vehicular Ad-Hoc networks," in *2014 8th International Conference on Complex, Intelligent and Software Intensive Systems*, Jul. 2014, pp. 44–49.
- [12] P. Sewalkar and J. Seitz, "Vehicle-to-Pedestrian communication for vulnerable road users: Survey, design considerations, and challenges," *Sensors*, vol. 19, no. 2, Jan. 2019.
- [13] O. Grembek, A. Kurzanskiy, A. Medury, P. Varaiya, and M. Yu, "Making intersections safer with I2V communication," *Transp. Res. Part C: Emerg. Technol.*, vol. 102, pp. 396–410, May 2019. [Online]. Available: <https://www.sciencedirect.com/science/article/pii/S0968090X19302566>
- [14] S. Zhang, M. Abdel-Aty, Y. Wu, and O. Zheng, "Pedestrian crossing intention prediction at Red-Light using pose estimation," *IEEE Trans. Intell. Transp. Syst.*, pp. 1–9, 2021.
- [15] H. O. Tezcan, M. Elmorssy, and G. Aksoy, "Pedestrian crossing behavior at midblock crosswalks," *J. Safety Res.*, vol. 71, pp. 49–57, Dec. 2019. [Online]. Available: <http://dx.doi.org/10.1016/j.jsr.2019.09.014>
- [16] X. Li and Y.-J. Wu, "Real-time estimation of pedestrian volume at button-activated midblock crosswalks using traffic controller event-based data," *Transp. Res. Part C: Emerg. Technol.*, vol. 122, p. 102876, Jan. 2021. [Online]. Available: <https://www.sciencedirect.com/science/article/pii/S0968090X20307762>
- [17] C. Zhang, B. Zhou, G. Chen, and F. Chen, "Quantitative analysis of pedestrian safety at uncontrolled multi-lane mid-block crosswalks in china," *Accid. Anal. Prev.*, vol. 108, pp. 19–26, Nov. 2017. [Online]. Available: <http://dx.doi.org/10.1016/j.aap.2017.08.018>
- [18] D. Eckhoff, C. Sommer, R. German, and F. Dressler, "Cooperative awareness at low vehicle densities: How parked cars can help see through buildings," in *2011 IEEE Global Telecommunications Conference - GLOBECOM 2011*, Dec. 2011, pp. 1–6.
- [19] C. Sommer, D. Eckhoff, and F. Dressler, "IVC in cities: Signal attenuation by buildings and how parked cars can improve the situation," *IEEE Trans. Mob. Comput.*, vol. 13, no. 8, pp. 1733–1745, Aug. 2014.
- [20] S. W. Loke, "Cooperative automated vehicles: A review of opportunities and challenges in socially intelligent vehicles beyond networking," *IEEE Transactions on Intelligent Vehicles*, vol. 4, no. 4, pp. 509–518, Dec. 2019.
- [21] R. Yee, E. Chan, B. Cheng, and G. Bansal, "Collaborative perception for automated vehicles leveraging Vehicle-to-Vehicle communications," in *2018 IEEE Intelligent Vehicles Symposium (IV)*, Jun. 2018, pp. 1099–1106.
- [22] X. Wu, S. Subramanian, R. Guha, R. G. White, J. Li, K. W. Lu, A. Bucci, and T. Zhang, "Vehicular communications using DSRC: Challenges, enhancements, and evolution," *IEEE J. Sel. Areas Commun.*, vol. 31, no. 9, pp. 399–408, Sep. 2013.
- [23] I. Standard, "Road vehicles—Controller Area Network (CAN) – part 1: Data link layer and physical signalling," *ISO*, vol. 11898, p. 1, 2003.
- [24] G. De Nicolao, A. Ferrara, and L. Giacomini, "Onboard Sensor-Based collision risk assessment to improve pedestrians' safety," *IEEE Trans. Veh. Technol.*, vol. 56, no. 5, pp. 2405–2413, Sep. 2007. [Online]. Available: <http://dx.doi.org/10.1109/TVT.2007.899209>
- [25] S. K. Kwon, E. Hyun, J.-H. Lee, J. Lee, and S. H. Son, "A Low-Complexity scheme for partially occluded pedestrian detection using LIDAR-RADAR sensor fusion," in *2016 IEEE 22nd International Conference on Embedded and Real-Time Computing Systems and Applications (RTCSA)*, Aug. 2016, pp. 104–104.
- [26] S. Zhang, J. Yang, and B. Schiele, "Occluded pedestrian detection through guided attention in cnns," in *Proceedings of the IEEE conference on Computer Vision and Pattern Recognition*, 2018, pp. 6995–7003.
- [27] Z. Chen and X. Huang, "Pedestrian detection for autonomous vehicle using Multi-Spectral cameras," *IEEE Transactions on Intelligent Vehicles*, vol. 4, no. 2, pp. 211–219, Jun. 2019.
- [28] A. Palffy, J. F. P. Kooij, and D. M. Gavrila, "Occlusion aware sensor fusion for early crossing pedestrian detection," in *2019 IEEE Intelligent Vehicles Symposium (IV)*, Jun. 2019, pp. 1768–1774.
- [29] C. Zhou, M. Yang, and J. Yuan, "Discriminative feature transformation for occluded pedestrian detection," in *Proceedings of the IEEE/CVF International Conference on Computer Vision*, 2019, pp. 9557–9566.
- [30] R. D. Brehar, M. P. Muresan, T. Marița, C.-C. Vancea, M. Negru, and S. Nedevschi, "Pedestrian Street-Cross action recognition in monocular far infrared sequences," *IEEE Access*, vol. 9, pp. 74 302–74 324, 2021. [Online]. Available: <http://dx.doi.org/10.1109/ACCESS.2021.3080822>
- [31] Y. He, C. Zhu, and X.-C. Yin, "Occluded pedestrian detection via Distribution-Based Mutual-Supervised feature learning," *IEEE Trans. Intell. Transp. Syst.*, pp. 1–16, 2021.
- [32] Y. Pang, J. Xie, M. H. Khan, R. M. Anwer, F. S. Khan, and L. Shao, "Mask-guided attention network for occluded pedestrian detection," in *Proceedings of the IEEE/CVF international conference on computer vision*, 2019, pp. 4967–4975.
- [33] M. Ding, W.-H. Chen, and Y. Cao, "Thermal infrared Single-Pedestrian tracking for advanced driver assistance system," *IEEE Transactions on Intelligent Vehicles*, pp. 1–1, 2022. [Online]. Available: <http://dx.doi.org/10.1109/TIV.2022.3140344>

- [34] P.-F. Ho and J.-C. Chen, "WiSafe: Wi-Fi pedestrian collision avoidance system," *IEEE Trans. Veh. Technol.*, vol. 66, no. 6, pp. 4564–4578, Jun. 2017. [Online]. Available: <http://dx.doi.org/10.1109/TVT.2016.2598786>
- [35] K. Dhondge, S. Song, B.-Y. Choi, and H. Park, "WiFiHonk: Smartphone-Based beacon stuffed WiFi Car2X-Communication system for vulnerable road user safety," in *2014 IEEE 79th Vehicular Technology Conference (VTC Spring)*, May 2014, pp. 1–5.
- [36] P. Wang, M. Zhou, and Z. Ding, "A VRU collision warning system with Kalman-Filter-Based positioning accuracy improvement," in *2021 IEEE International Conference on Information Communication and Software Engineering (ICICSE)*, Mar. 2021, pp. 191–198.
- [37] S. Hisaka and S. Kamijo, "On-board wireless sensor for collision avoidance: Vehicle and pedestrian detection at intersection," in *Proc. 14th IEEE International Conference on Intelligent Transportation Systems (ITSC)*, 2011, pp. 198–205.
- [38] R. Zhang, L. Song, A. Jaiprakash, T. Talty, A. Alanazi, A. Alghafis, A. A. Biyabani, and Ozan Tonguz, "Using Ultra-Wideband technology in vehicles for infrastructure-free localization," in *2019 IEEE 5th World Forum on Internet of Things (WF-IoT)*, Apr. 2019, pp. 122–127.
- [39] A. Tahmasbi-Sarvestani, H. Nourkhiz Mahjoub, Y. P. Fallah, E. Moradi-Pari, and O. Abuchaar, "Implementation and evaluation of a cooperative vehicle-to-pedestrian safety application," *IEEE Intelligent Transportation Systems Magazine*, vol. 9, no. 4, pp. 62–75, 2017.
- [40] P. Merdrignac, O. Shagdar, and F. Nashashibi, "Fusion of perception and V2P communication systems for the safety of vulnerable road users," *IEEE Trans. Intell. Transp. Syst.*, vol. 18, no. 7, pp. 1740–1751, Jul. 2017.
- [41] P. Sun and A. Boukerche, "A novel Internet-of-Vehicles assisted collaborative low-visible pedestrian detection approach," in *GLOBECOM 2020 - 2020 IEEE Global Communications Conference*, Dec. 2020, pp. 1–6.
- [42] M. Islam, M. Rahman, M. Chowdhury, G. Comert, E. D. Sood, and A. Apon, "Vision-Based personal safety messages (PSMs) generation for connected vehicles," *IEEE Trans. Veh. Technol.*, vol. 69, no. 9, pp. 9402–9416, Sep. 2020.
- [43] A. Ben Khalifa, I. Alouani, M. A. Mahjoub, and A. Rivenq, "A novel multi-view pedestrian detection database for collaborative intelligent transportation systems," *Future Gener. Comput. Syst.*, vol. 113, pp. 506–527, Dec. 2020. [Online]. Available: <https://www.sciencedirect.com/science/article/pii/S0167739X20300340>
- [44] B. Noh and H. Yeo, "A novel method of predictive collision risk area estimation for proactive pedestrian accident prevention system in urban surveillance infrastructure," *Transportation Research Part C: Emerging Technologies*, vol. 137, p. 103570, 2022.
- [45] T. Larson, A. Wyman, D. S. Hurwitz, M. Dorado, S. Quayle, and S. Shetler, "Evaluation of dynamic passive pedestrian detection," *Transportation Research Interdisciplinary Perspectives*, vol. 8, p. 100268, Nov. 2020.
- [46] J. Zhao, H. Xu, H. Liu, J. Wu, Y. Zheng, and D. Wu, "Detection and tracking of pedestrians and vehicles using roadside LiDAR sensors," *Transp. Res. Part C: Emerg. Technol.*, vol. 100, pp. 68–87, Mar. 2019.
- [47] F. Pereira, H. Sampaio, R. Chaves, R. Correia, M. Luís, S. Sargento, M. Jordão, L. Almeida, C. Senna, A. S. R. Oliveira, and N. Borges Carvalho, "When backscatter communication meets vehicular networks: Boosting crosswalk awareness," *IEEE Access*, vol. 8, pp. 34 507–34 521, 2020.
- [48] A. Senart, M. Karpinski, M. Wieckowski, and V. Cahill, "Using sensor networks for pedestrian detection," in *2008 5th IEEE Consumer Communications and Networking Conference*, Jan. 2008, pp. 697–701. [Online]. Available: <http://dx.doi.org/10.1109/ccnc08.2007.160>
- [49] N. Liu, M. Liu, W. Lou, G. Chen, and J. Cao, "PVA in VANETs: Stopped cars are not silent," in *2011 Proceedings IEEE INFOCOM*, Apr. 2011, pp. 431–435.
- [50] S. Abdelhamid, H. S. Hassanein, and G. Takahara, "Vehicle as a resource (vaar)," *IEEE Network*, vol. 29, no. 1, pp. 12–17, 2015.
- [51] W. M. Griggs, R. Verago, J. Naoum-Sawaya, R. H. Ordóñez-Hurtado, R. Gilmore, and R. N. Shorten, "Localizing missing entities using parked vehicles: An RFID-Based system," *IEEE Internet of Things Journal*, vol. 5, no. 5, pp. 4018–4030, Oct. 2018. [Online]. Available: <http://dx.doi.org/10.1109/JIOT.2018.2864590>
- [52] J. Zhao and Z. You, "A shoe-embedded piezoelectric energy harvester for wearable sensors," *Sensors*, vol. 14, no. 7, pp. 12 497–12 510, Jul. 2014.
- [53] Q. Huang, Y. Mei, W. Wang, and Q. Zhang, "Toward Battery-Free wearable devices: The synergy between two feet," *ACM Trans. Cyber-Phys. Syst.*, vol. 2, no. 3, pp. 1–18, Jun. 2018.
- [54] A. Zanella, "Best practice in RSS measurements and ranging," *IEEE Communications Surveys Tutorials*, vol. 18, no. 4, pp. 2662–2686, 2016. [Online]. Available: <http://dx.doi.org/10.1109/COMST.2016.2553452>
- [55] T. Stoyanova, F. Kerasiotis, and G. Papadopoulos, "RSS-Based outdoor localization with wireless sensor networks in practice," in *Technological Breakthroughs in Modern Wireless Sensor Applications*. IGI Global, 2015, pp. 225–256. [Online]. Available: <https://www.igi-global.com/chapter/rss-based-outdoor-localization-with-wireless-sensor-networks-in-practice/129223>
- [56] S. Seneviratne, Y. Hu, T. Nguyen, G. Lan, S. Khalifa, K. Thilakarathna, M. Hassan, and A. Seneviratne, "A survey of wearable devices and challenges," *IEEE Communications Surveys Tutorials*, vol. 19, no. 4, pp. 2573–2620, 2017. [Online]. Available: <http://dx.doi.org/10.1109/COMST.2017.2731979>
- [57] J. Balen, G. Martinovic, K. Paridel, and Y. Berbers, "PVCN: Assisting multi-hop communication in vehicular networks using parked vehicles," in *2012 IV International Congress on Ultra Modern Telecommunications and Control Systems*, Oct. 2012, pp. 119–122.
- [58] S. Olariu and M. C. Weigle, Eds., *Vehicular Networks: From Theory to Practice*. CRC Press/Taylor & Francis, March 2009.
- [59] M. Aljohani, S. Olariu, A. Alali, and S. Jain, "A survey of parking solutions for smart cities," *IEEE Trans. Intell. Transp. Syst.*, vol. 23, no. 8, pp. 10 012–10 029, Aug. 2022. [Online]. Available: <http://dx.doi.org/10.1109/TITS.2021.3112825>
- [60] D. Sam, C. Velanganni, and T. E. Evangelin, "A vehicle control system using a time synchronized hybrid vanet to reduce road accidents caused by human error," *Vehicular Communications*, vol. 6, pp. 17–28, 2016. [Online]. Available: <https://www.sciencedirect.com/science/article/pii/S2214209615300139>
- [61] Y. T. Lo and S. Lee, *Antenna Handbook: theory, applications, and design*. Springer Science & Business Media, 2013.
- [62] R. Koppa, "Human factors," 2003. [Online]. Available: <https://www.fhwa.dot.gov/publications/research/operations/tft/chap3.pdf>
- [63] P. A. Lopez, M. Behrisch, L. Bieker-Walz, J. Erdmann, Y.-P. Flötteröd, R. Hilbrich, L. Lücken, J. Rummel, P. Wagner, and E. Wießner, "Microscopic traffic simulation using sumo," in *The 21st IEEE International Conference on Intelligent Transportation Systems*, 2018, pp. 2575–2582.
- [64] T. Stoyanova, F. Kerasiotis, K. Efsthioiu, and G. Papadopoulos, "Modeling of the RSS uncertainty for RSS-Based outdoor localization and tracking applications in wireless sensor networks," in *2010 Fourth International Conference on Sensor Technologies and Applications*. ieeexplore.ieee.org, Jul. 2010, pp. 45–50. [Online]. Available: <http://dx.doi.org/10.1109/SENSORCOMM.2010.14>
- [65] M. Arif, G. Wang, Z. A. Bhuiyan, T. Wang, and J. Chen, "A survey on security attacks in VANETs: Communication, applications and challenges," *Vehicular Communications*, vol. 19, p. 100179, Oct. 2019. [Online]. Available: <https://www.sciencedirect.com/science/article/pii/S2214209619302268>
- [66] S. Olariu, A. Wadaa, L. Wilson, and M. Eltoweissy, "Wireless sensor networks: leveraging the virtual infrastructure," *IEEE Netw.*, vol. 18, no. 4, pp. 51–56, Jul. 2004.
- [67] S. El-Tawab, S. Olariu, and M. Almalag, "FRIEND: a cyber-physical system for traffic flow related information aggregation and dissemination," in *Proc. IEEE World of Wireless, Mobile and Multimedia Networks (WoWMoM'2012)*, San Francisco, June 2012, pp. 1–6.
- [68] G. Yan, S. Olariu, and D. C. Popescu, "NOTICE: An Architecture for the Notification of Traffic Incidents," *IEEE Intelligent Transportation Systems Magazine*, vol. 4, no. 4, pp. 6–16, Winter 2012.
- [69] S. El-Tawab, A. Alhafidhi, D. Treeumnuk, D. C. Popescu, and S. Olariu, "Physical layer aspects of information exchange in the NOTICE architecture," *IEEE Intelligent Transportation Systems Magazine*, vol. 7, no. 1, pp. 8–18, 2015.

## APPENDIX

### A. The time-space diagram

One of the basic tools in the tool-box of traffic engineers is the *time-space diagram* that allows one to plot the trajectories of vehicles as curves in a Cartesian plane with axes labeled "time" and "space". Referring to Figure 19, the vehicle's coordinates at time  $t$  are  $(t, s)$ . The projection of this point on the vertical axis,  $(0, s)$ , indicates the position, at time  $t$ , of

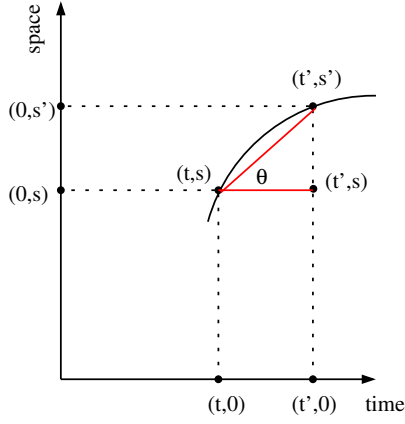


Fig. 19: Illustrating the time-space diagram.

a vehicle that moves along the space axis North-bound (i.e. from bottom to top).

Assume that the same vehicle has continued moving along its trajectory in such a way that at time  $t'$ , ( $t' > t$ ), its coordinates in the time-space coordinate system are  $(t', s')$ . Equivalently, in the time interval  $[t, t']$ , the vehicle has moved along the space axis from location  $(0, s)$  to location  $(0, s')$ .

One of the nice features of the time-space diagram is that it allows one to compute and to *visualize* the average speed of the vehicle. Indeed, referring again to Figure 19, elementary physics indicate that the average speed,  $v_{avg}$ , of the vehicle in the time interval  $[t, t']$  is the ratio

$$v_{avg} = \frac{s' - s}{t' - t}. \quad (19)$$

This is the same as the *slope* of the line segment connecting the points of coordinates  $(t, s)$  and  $(t', s')$ . Equivalently, the average speed  $v_{avg}$  is  $\tan(\theta)$ , where  $\theta$  is the angle determined by the line segment connecting the points of coordinates  $(t, s)$  and  $(t', s')$  and the positive direction of the time axis.

Finally, it is not hard to see that the *instantaneous speed* of the vehicle at an arbitrary time  $\tau$ , ( $t \leq \tau \leq t'$ ) turns out to be the slope of the tangent to the trajectory at time  $\tau$ . In particular, if the trajectory happens to be a straight line, then the average speed matches the instantaneous speed, as expected.

### B. Time-space diagram of a crossing cohort

Let us turn our attention to the time-space diagram corresponding to a crossing cohort. Referring to Figure 20, imagine a crossing cohort at location  $L$  that starts crossing the street at time  $s1$  and clears the street by time  $e1$ . Since the “space” coordinate of the cohort does not change, the corresponding time-space diagram is captured by a horizontal line segment with endpoints  $(s1, L)$  and  $(e1, L)$ .

Now, consider an approaching car and assume that the coordinates of the car when it receives the “Caution – pedestrian in the street” message are  $(s1, C)$ . What is the largest average speed that the approaching car should adopt to avoid crashing into the cohort? The answer is simple: the car should not reach the point  $(0, L)$  while the crossing is in progress, namely in

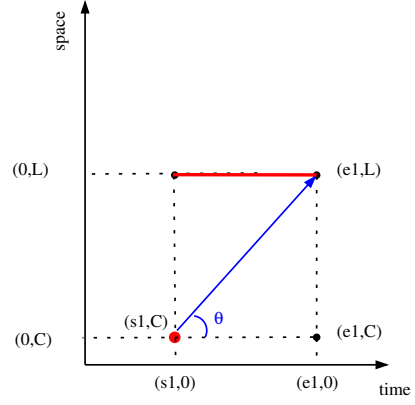


Fig. 20: Illustrating the time-space diagram of a crossing pedestrian.

the time interval  $[s1, e1]$ . However, the car may reach  $(0, L)$  at time  $e1$ , as by that time the cohort has finished crossing safely. Thus, using (19), the car should adopt the following *safe average speed*:

$$v_{safe} = \min \left\{ v_{max}, \frac{L - C}{e1 - s1} \right\} \quad (20)$$

where  $v_{max}$  is the speed limit on the road considered. Assuming that  $\frac{L-C}{e1-s1} \leq v_{max}$ , this safe speed is visualized in Figure 20 as the slope of the blue segment connecting the points  $(s1, C)$  and  $(e1, L)$ .